



Published in final edited form as:

Toxicol Appl Pharmacol. 2020 August 01; 400: 115041. doi:10.1016/j.taap.2020.115041.

World Trade Center Dust Induces Airway Inflammation while Promoting Aortic Endothelial Dysfunction

Michelle Hernandez, Andrea Harrington, Yanqin Ma, Karen Galdanes, Beth Halzack, Mianhua Zhong, Joshua Vaughan, Ethan Sebasco, Terry Gordon, Morton Lippmann, Lung Chi Chen

Department of Environmental Medicine, New York University School of Medicine, New York, NY 10010

Abstract

Respiratory ailments have plagued occupational and public health communities exposed to World Trade Center (WTC) dust since the September 11, 2001 attack on the Twin Towers. The nature of these ailments is proposed to be induced by inhalation exposure to WTC particulate matter (WTC_{PM}), released during the collapse of the buildings and subsequent resuspension during cleanup. We investigated this hypothesis using both an *in vitro* and an *in vivo* mouse intranasal (IN) exposure model to identify the inflammatory potential of WTC_{PM} with specific emphasis on respiratory and endothelial tissue responses. *In vitro* studies identified WTC_{PM} exposure to be positively correlated with cytotoxicity and increased NO₂⁻ production in both BEAS-2B pulmonary epithelial cells and THP-1 macrophage cells. *In vivo* C57BL/6 mouse studies exhibited significant increases in inflammatory markers including increases in polymorphonuclear neutrophil (PMN) influx into nasal and bronchoalveolar lavage fluids (NLF and BALF), as well as increased total protein and cytokine/chemokines levels. Concurrently, NLF, BALF, and serum NO₂⁻ levels exhibited significant homeostatic temporal deviations with evidence of temporal aortic dysfunction in myography studies. Respiratory exposure to- and evidence -based retention of- WTC_{PM} may contribute to chronic systemic effects seen in mice, with resemblance to observed effects in WTC_{PM}-exposed human populations. Collectively, findings reported herein are reflective of WTC_{PM} exposure and its effect(s) on respiratory and aortic tissues, highlighting potential dysfunctional pathways that may precipitate inflammatory events, while simultaneously altering homeostatic balances. The tight interplay between these balances, when chronically altered, may contribute to- or result in- chronically diseased pathological states.

Address correspondence to LC Chen, 341 E. 25th St., New York, NY 10010 USA, Telephone: (646) 754-9453, lcc4@nyu.edu. Authors' contributions: MH conceived, designed, coordinated, and performed all experiments, as well as statistical analyses and manuscript drafts. AH and YM assisted with and performed vascular myography and data interpretation. KG, BH, MZ, JV, and ES assisted in sample preparation and analysis. TG, ML, and LCC assisted in study design and manuscript editing. All authors read and approved the final manuscript.

Publisher's Disclaimer: This is a PDF file of an article that has undergone enhancements after acceptance, such as the addition of a cover page and metadata, and formatting for readability, but it is not yet the definitive version of record. This version will undergo additional copyediting, typesetting and review before it is published in its final form, but we are providing this version to give early visibility of the article. Please note that, during the production process, errors may be discovered which could affect the content, and all legal disclaimers that apply to the journal pertain.

Data Statement

Availability of data and material: The datasets used and/or analyzed during the current study are available from the corresponding author on reasonable request.

Keywords

World Trade Center dust; particulate matter exposure; inhalation toxicology; intranasal instillation; pulmonary inflammation; endothelial cell dysfunction

Background

Over a million tons of debris and airborne particulate matter (PM) were generated and/or removed from the World Trade Center (WTC) site within the first year after the collapse, exposing an estimated 400,000+ people, including first responders, residents, and workers engaged in the massive cleanup and building maintenance [1]. The debris, comprised of building materials, furniture and office equipment combustion residues, paper, and unburned jet fuel, were incorporated into WTC_{PM} during the collapse event [2]. No single element, compound, or factor has been implicated as being causal for the observed adverse health effects in WTC_{PM}-exposed human populations, but PM chemical composition and alkalinity can potentially provide links between exposure and subsequent symptoms that have been associated with WTC_{PM} exposure, or in relation to causality for the degradations of cellular and systemic response pathways. Some symptoms associated with more conventional ambient air PM exposure have been similar to those experienced by people exposed to WTC_{PM} and may be indicative of a common factor between PM exposure and WTC_{PM} exposure. Epidemiologic studies have demonstrated relationships between WTC_{PM} exposure and adverse health outcomes experienced by rescue workers and residents of the surrounding area and were found to be dominated by lower respiratory symptoms similar to those who suffer from PM exposure (coughing, wheezing, and aggravated asthma) [3].

Previous particle characterization studies have indicated WTC_{PM} to be highly alkaline (pH 9.2-12), derived from the compositional makeup of the dust with 50% being comprised of an alkaline mixture containing cement and gypsum dust and the other 40% being synthetic vitreous fibers [SVF]). Conventional ambient air PM respiratory effects studies have focused on neutral and/or acidic respirable particles <2.5 μm in aerodynamic diameter to identify the potential adverse respiratory effects. Uniquely, >99% of WTC_{PM} were >10 μm , with 59.1% of the PM mass ranging in size from 10-53 μm [4,5]. Due to compositional similarities between fractional size groups greater than 2.5 μm , physiological responses to such coarse particles would likely be due to respiratory tract deposition patterns that vary with particle size, whereby coarse thoracic PM (2.5 – 10 μm) and super-coarse (10-53 μm) fractions deposit most prevalently in the conductive airways of the upper respiratory tract and tracheobronchial tree, where sensory innervations are more dominant.

The conductive airways provide the first line of defense against inhaled PM, specifically maintained by their characteristic structural configurations, mucosal surfaces, prevalent innate immune cells, and antioxidant rich environment. However, WTC_{PM} exposures, particularly in the context of WTC First Responders, can overwhelm defensive capabilities, leaving the upper- and potentially lower-respiratory tract vulnerable. Understanding the interplay between particle retention and clearance mechanisms can determine appropriate courses of action and treatment for those exposed to WTC_{PM}. Considering WTC_{PM} is a

highly heterogeneous mixture, conventional applications of treatment may or may not be successful considering the multitude and array of particles being exposed to the respiratory systems, and potentially other systems directly or indirectly.

The objective of this study was to investigate WTC_{PM} exposure and its role in inflammatory potentiation in both *in vitro*-cell and *in vivo*-mouse models, with specific emphasis on respiratory cardiovascular tissues. Investigating these interactions at the nasal-pulmonary interface can help illuminate long-term health issues associated with generic PM exposures, including central nervous system effects and/or co-exposure effects from the surrounding cleanup area.

To achieve an exposure method with relevance for human health outcomes, this study implemented intranasal (IN) instillation as a particle delivery mechanism based on the ability of these large alkaline particles to not only be deposited in the nasal cavity, but to also be aspirated into lower pulmonary areas. This exposure methodology provides a real-world exposure scenario based on the high potential for the overloading of particle clearance capacity, in both nasal and pulmonary tissues, that may have occurred in people caught in the dense WTC_{PM} plume. This research is critical to understanding causal mechanisms and/or events that may precipitate inflammatory cascades that, if occurring chronically, could shed light on processes involved in pulmonary and extra-pulmonary disease development.

Methods

***In vitro* Cell Lines:**

BEAS-2B (ATCC®, Manassas, VA) cells were maintained in complete media containing Dulbecco's Modified Eagle Medium (DMEM) according to manufactures protocol and seeded at $15\text{-}30 \times 10^4$ cells/cm². THP-1 cells (ATCC®, Manassas, VA) were maintained in suspension cultures containing complete RPMI 1640 media and seeded at densities of $2\text{-}4 \times 10^4$ cells/ml. Addition of PMA in DMSO (Sigma-Aldrich®, St. Louis, MO) was accomplished at a final concentration of 0.1% in media, with cells assayed 3 days post-PMA exposure. Cultures were maintained at 37°C in a humidified 5% CO₂ atmosphere.

CytoTox 96 Non-Radioactive Cytotoxicity Assay:

CytoTox 96® Non-Radioactive cytotoxicity assay kit (Promega, USA) was used in accordance with manufacturer protocol. Lysis 10X Solution (9% (v/v) Triton®X-100 in water) was provided by the manufacturer for use as the positive control. Cytotoxicity percentage was calculated using the formula provided by the manufacturer (% cytotoxicity = [Abs of experimental sample/ Abs of maximum LDH release] x 100).

Colony Formation Unit Assay:

BEAS-2B cells were harvested and seeded at 300-400 cells per dish and incubated for 24 hours with addition of treatment media (31 µg-1 mg/ml of WTC_{PM}). Cells were stained with 0.5% crystal violet and visible colonies were counted after a 10-day incubation. Colonies were considered strong for scoring with 50 cells/colony.

Griess Reagent System:

Cell-free mouse NLF, BALF, and hemolysis-free serum were assayed using the Griess Reagent System (Promega, Madison, WI) and prepared according to manufacturer protocol. Concentrations of total nitrite were calculated from a standard curve established with serial dilutions of sodium nitrite starting at 100 μM and ending at 0.39 μM , with a limit of detection of 2.5 μM . Colorimetric optical density was read at 535 nm.

Animals:

Pathogen-free 8-10-week old and age-matched control male C57BL/6 mice were purchased from The Jackson Laboratory (Bar Harbor, ME). All animals were housed in an approved facility at NYUSOM and acclimated for 1-2 weeks under controlled temperature ($22 \pm 2^\circ\text{C}$) and relative humidity (30-50%) with a 12-hr light/ dark cycle prior to use in any experiments. Mice were provided *ad libitum* access to standard laboratory chow and filtered water. All protocols were approved by the NYU School of Medicine IACUCs.

Intranasal Instillation:

Mice were anesthetized in a closed container with 1-3% Isoflurane in oxygen (Butler Schein, Dublin, OH). Mice were affixed to a plexiglass board at a 45° angle. Top and bottom incisors were secured, and particle suspension delivered in a volume of 50 μl . Exposure frequency included a single IN instillation or 4 IN instillations over the course of one week (day 1, day 3, day 5 and day 7).

WTC_{PM} Particle Preparation:

Concentrations of 31 μg -1000 $\mu\text{g}/\text{ml}$ were prepared from dry WTC_{PM10-53 μm} or WTC_{PM<53 μm} stocks and suspended in media 1 hour prior to *in vitro* exposures. For the purposes of the studies herein, all *in vivo* studies were performed with DPBS-suspended WTC_{PM<53}. Doses ranging from 31 μg – 4000 $\mu\text{g}/50$ μl were prepared from dry WTC_{~53 μm} dust stocks and suspended in DPBS (or water for alkalinity studies) 1 hour prior to *in vivo* IN instillations. For alkalinity studies, sodium hydroxide pellets (Sigma-Aldrich®, St. Louis, MO) were dissolved in sterile water and diluted to 1.0 μM at a pH of 8.1, sterile filtered and intranasally instilled at 50 μl .

Animal Processing Post-Exposure:

Intranasally instilled animals were euthanized 24hours-post single or final exposure via intraperitoneal injection of pentobarbital (0.36mg/g). Serum, bronchoalveolar lavage fluid (BALF), nasal lavage fluid (NLF), whole lung and nasal cavities were collected and stored at -80°C . Of note, the nasal cavities is inclusive of the area from the cribriform plate to the nares, to include the ethmoturbinates, nasoturbinates, maxilloturbinates, and nasal vestibule. Whole blood collected from the vena cava was centrifuged at 3000 x g for 10 minutes. Serum was collected, double spun, isolated, and stored at -20°C to be evaluated for nitrite. Triple flush BALF and NLF samples using Dulbecco's phosphate-buffered saline (DPBS, pH 7.4) were collected and placed at 4°C . Lavage fluids were centrifuged (15,000 x g for 5 minutes) for generation of cell-free supernatant and stored at -20°C for endpoint evaluation. For transpharyngeal nasal lavages, head and mandible were excised and cannula inserted

into the posterior opening of the pharynx for nasal cavity flushing. Organs and intact nasal cavities were weighed, flash frozen in liquid nitrogen and stored at -80°C . For histopathologic valuations, lungs were fixed *in situ* with 10% formalin at a constant fluid pressure of 25cm. Whole lungs sections were processed and stained with H&E or PAS. All pulmonary tissues were semi-quantitatively evaluated by a certified histopathologist (Mass Histology Associates, Inc.; Worcester, MA), and graded accordingly to an endpoint: N/0= Normal; 1= Minimal; 2= Mild; 3= Moderate; 4=Severe.

Cellular Differentials and Cell Counts:

Differential slides were affixed with 100 μl of BALF or NLF, fixed in methanol and stained with Hemacolor (Harleco, Gibbs-town, NJ). Differential cell counts were performed under light microscopy with cells totals determined via hemocytometer. Cell viability was evaluated using Trypan blue staining (Sigma-Aldrich®, St. Louis, MO).

Total Protein Assay:

Epithelial permeability was assessed by the Bradford method, quantifying levels of total protein in BALF and NLF using a Coomassie Blue protein assay (Thermo Scientific, West Palm Beach, FL). Cell-free supernatant total protein was measured at an absorbance of 595 nm.

Enzyme-Linked Immunosorbent Assays (ELISA):

Protein levels of mouse TH1, TH2, and TH17 cytokines/chemokines from BALF and NLF (n=5; samples pooled) were determine using a MultiAnalyte ELISArray kit (Qiagen) according to manufacturer's instructions. Colorimetric quantitation of 570 nm and 450 nm optical densities were used to adjust for wavelength correction. Reported ELISA values are relative optical density percentages relative to control mean values.

Inductively coupled plasma mass spectrometry (ICP-MS):

Whole lungs and nasal cavities were excised and trimmed for determination of wet/dry weight ratios as well as trace elemental analysis (Perkin Elmer NexION 350D) undergoing standardized drying and digestion protocols (Titan MPS Microwave) using tissue specific programs, and with Sc, In and TB serving as internal standards. Results are given in $\mu\text{g/g}$ of dried tissue calculated by ICP-MS Syngistix V1.1 software.

Vascular Function and Graded Dose Responses:

Aortic pharmacological response was performed 1, 7, and 30 days following a single vehicle or single WTC_{PM} intranasal exposure. The thoracic aorta was excised, perivascular adipose tissue removed, and 2 mm cylindrical sections mounted onto myography chamber pins (DMT620M multi-channel myography system; DMT, Ann Arbor, MI) in a continuously oxygenated bath per standard assay procedures [6]. Standard incubation challenges were employed and drug stock concentrations of phenylephrine (PE) and acetylcholine (Ach) (Sigma-Aldrich®, St. Louis, MO) were administered in ascending concentrations. Vascular contractility was expressed as a percentage of the peak response to 100 mM KPSS. Half-

maximal dilation and contraction values and maximum contraction and relaxation values were used to compare treatment groups [7].

Statistical Analyses:

Statistical Analyses were performed using GraphPad Prism® software (Version 5.0, GraphPad Software Inc.) or Microsoft Excel. All data are expressed as mean \pm SEM. An unpaired t-test was used to determine differences within treatment groups with respect to the various intranasal treatments and control treatments. A one-way analysis of variance (ANOVA) with a Student-Newman-Keul's post-hoc analysis was used to determine significant differences associated with multiple exposure groups as well as control groups. A repeated-measures two-way ANOVA with Bonferroni's post-tests was used to evaluate vascular reactivity with respect to pharmacologic testing. Dixon and Grubbs analyses were used to screen for outliers. Differences were interpreted as statistically significant when p-values were below the threshold of 0.05.

Results

WTC_{PM} induces *in vitro* cytotoxicity in structural and immunologic cells

In vitro methods using BEAS-2B and THP-1 cell lines were employed to preliminarily investigate the cytotoxic potential of WTC_{PM10-53} and WTC_{PM<53} particle size groups, via LDH release, NO₂⁻ formation and colony formation. Figure 1A demonstrates increased LDH release in BEAS-2B bronchial epithelial cells with increasing WTC_{PM} concentrations in cell culture media. In comparison to control cells, LDH release increased from approximately 7% at 31 μ g/ml to 35-50% at 1000 μ g/ml across both particle size groups, with R² values of 0.82 and 0.73 for 10-53 μ m and <53 μ m groups, respectively. Figure 1B illustrates a positive correlation (R²=0.94) between increased BEAS-2B LDH production and increased NO₂⁻ production, as well as dose-dependent decreased colony formation units in Figure 1C, ranging from 93% clonogenic ability at 31 μ g/ml down to 0% at both 500 and 1000 μ g/ml. Similarly, THP-1 monocytes showed a dose-dependent increase in NO₂⁻ production (Figure 1D).

WTC_{PM} induces respiratory tract inflammation *in vivo*

Figures 2 A and B illustrate significant neutrophil influx in both upper and lower respiratory tissues of mice treated with WTC_{PM} in single or multiple intranasal instillations (IN). Nasal PMN infiltrates significantly increased from control baseline (~3%) to approximately 20-25% PMNs in single exposure dose categories of 125 – 1000 μ g. Similarly, pulmonary % PMN influx was significantly increased at doses >31 μ g. In comparing single and multiple dose groups, some groups receiving multiple IN instillations were found to have decreased % PMN influx relative to mice receiving the same dose in a single IN instillation (Supplemental Figure 1). In a 24-hour time course evaluation, mice exposed to a single dose of 125 μ g WTC_{PM} experienced peak NLF and BALF PMN influx 24 hours and 6 hours post-exposure, respectively (Figures 2C and D). In BALF, total cell count peak (5.9 x 10⁴ total cells) coincided with PMN influx (50%) and protein increases (17000 μ g/ml). ELISArray data in Figures 2E and F identify significantly increased cytokines in NLF (IL1 α , IL2, IL12, IL17A, TNF α and GM-CSF) and BALF (IL1 α , IL2, IL4, IL6, IL12, IL17A, TNF α , G-vFSF

and GM-CSF) in mice 24 hours after a single exposure to 250 or 1000 μg of WTC_{PM} . With regards to short- and long-term pulmonary injury indicators, wet/dry ratios (indicative of lung edema) were significantly higher in single exposure WTC_{PM} treated mice 24 hours post-exposure (Supplemental Figure 2). While data indicate dissipation of edema at 30 days post-exposure, a single treatment of 1000 μg WTC_{PM} contributed to an 11% decrease in viable alveolar macrophages 30 days post-exposure (Supplemental Figure 3).

Alkalinity, particles or metals as toxicity factors

With reference to pH, DPBS-suspended WTC particle pH remained neutral with a pH range of 6.8-7.3 (Figure 3A). Conversely, water-suspended particles exhibited a pH dependent increase in relation to increased WTC_{PM} concentrations, ranging from 6.5-10. Use of three different WTC_{PM} concentrations suspended in water (reflective of low, medium, and high pH) or DPBS (reflective of neutralized pH), identified BALF PMN influx differences between water and DPBS groups, with PMNs remaining similar across water-suspended groups (15-19% PMN) and varied in DPBS-suspended groups (9-39% PMN) (Figure 3B). In NLF, nitrite levels of water suspended WTC_{PM} remained unchanged from control values. In medium (125 μg) and high dose (1000 μg) DPBS-suspended group, NLF total nitrite levels were significantly increased ($\sim 25\mu\text{M}$) as compared to the DPBS control group (7 μM) (Figure 3C). Conversely, BALF total nitrite levels significantly decreased in a dose dependent manner regardless of suspending vehicle (Figure 3D). Figure 3E further identifies WTC particles to be the main influencing toxicity factor with the most robust PMN response had by the DPBS-suspended (pH neutralized) WTC particle group. Evidence of particle penetration and retention into the upper and lower airways 24 hours and 90 days post-single exposure can be seen in Figures 4A and B. Graded pulmonary tissues collected 30 days post- WTC_{PM} exposure revealed minor to mild inflammation, no increased mucus production or fibrotic formations (Supplemental Figure 4 and Supplemental Table 1). Analysis of pulmonary insoluble and soluble particles revealed lung burden increases of Al (3964%), Cr (1172%), Ca (284%) and Mn (479%). Pulmonary levels of Al, Ti, Cr, Pb, Ba, Sr, Zn, Cu, Mo, Na, Mg, Ca, Mn, and Ni were all found to be significantly increased in higher exposure concentration groups of 1000 μg (data not shown) and 4000 μg (Figures 5A and B).

Potential indications of long-term effects on other organ systems

Preliminary BALF and serum total nitrite data in Figures 6A and B illustrate significantly lower levels of BALF and serum nitrite 24 hours post- WTC_{PM} exposure. A more than doubling of BALF and serum total nitrite occurred in the 1000 μg exposure group 90 days post-exposure, as compared to controls. Figures 7A–C identifies maximum aortic contraction responses to phenylephrine (PE) as well as maximum relaxation responses to acetylcholine (Ach) in WTC_{PM} exposed mice at 24 hours, 7 days, and 30 days post single WTC_{PM} exposure. Figure 7A illustrates a lack of difference between control and WTC_{PM} exposed mice against increasing concentrations of PE and Ach, respectively, 24 hours post- WTC_{PM} exposure. Aortas tested 7 days post- WTC_{PM} exposure began exhibiting differences between WTC exposed and control groups with a more definitive difference between maximum PE and Ach responses (Figure 7B). These changes remained statistically insignificant, although differences in % change were larger between control and WTC_{PM} exposed groups. This relationship is more evident and sustained 30 days post-exposure,

whereby vessel relaxation values are significantly different from control aortic vessel values at -7 , -6 , and -5 M concentrations of PE and Ach, with approximately a 35% difference between control and WTC_{PM} exposed groups (Figure 7C). ICP-MS data from whole hearts revealed significant decreases in soluble Mg, K, Mn, Cr, and Zn and increased Cu, As, Se, P, and Ca and K in animals sacrificed 24 hours post-exposure as well as 30 days post-exposure (Supplemental Figures 5 and 6).

Discussion

The WTC_{PM} exposure event was not a single exposure event, but a multiple exposure event, with continuous exposures through rescue/recovery operations, working on the central pile which burned well into early October 2001, and the year-long outdoor and indoor clean-up phases which are less well documented. Thus, formal human exposure estimates have not been identified, but have been categorized by amount of time spent occupationally on the WTC pile. Aside from a lack of understanding with regards to human dosimetry estimates, many challenges remain regarding routes of exposure, duration, ventilation rates, frequency, locality/temporality, temperature, and other forms of exposure.

Previous WTC_{PM} *in vitro* studies revealed exposure to WTC_{PM10-53} increased inflammatory cytokine production in alveolar macrophages obtained from human subjects without WTC-exposure or pulmonary symptoms and suggested the large particle exposure may have contributed to the high incidence of lung injury in WTC exposed populations [8]. Cytotoxicity endpoints, including decreased cellular viability and increased apoptotic activity in pulmonary fibroblasts were also reported at doses similar to those tested in this study [9]. Initial rodent *in vivo* investigations examining WTC induced health effects were begun by Gavett et al., briefly 2 years after the collapse of the towers, and followed up by studies published by Cohen et al. and Vaughan et al., and culminating in a review of literature published by Lippmann et al. [10–12, 3]. The studies herein continue the investigation into respiratory and endothelial tissue impacts with evaluations focused at the nasal-pulmonary interface, identifying increased inflammatory parameters derived from WTC_{PM} exposure. The design of these assessments were based on previous WTC human health studies demonstrating a link between disease development, oxidative and inflammatory potentials of the dust itself. The data and information provided conclusively demonstrate nasal and pulmonary inflammation follow WTC_{PM} exposure. The mechanisms behind inflammatory outcomes may be related to respiratory oxidant stressors, brought about by a surplus of reactive electrophiles, mainly by both resident (epithelial and endothelial) cells and infiltrated leukocytes, all of which have been found to play substantial roles in tissue injury and abnormal tissue repair.

WTC_{PM} was found to be cytotoxic and induced nitritive stress parameters in pulmonary derived cells (BEAS-2B) and immunologic monocytic cells lines (THP-1). These *in vitro* parameters proved to be dose specific, supporting the idea that structural cells, as well as immunologic cells within pulmonary pathways may very well have been adversely affected in the WTC_{PM} exposure event. Typically, in normal and uninjured alveoli, a major part of the surface area is comprised of type I epithelial cells and cuboidal type II cells that are involved in surfactant production, fluid transport, and repopulation of the alveolar

epithelium post-injury. In injured alveoli, the epithelia undergo apoptotic/necrotic events, basement membrane denudation, inflammatory cell influx, as well as macrophage and PMN activation [13,14]. During these events, proteases, oxidants, cytokines/ chemokines, and other inflammatory mediators are released, coupled with protein-rich fluid influx into the alveolar spaces. Many of these events have been documented within the scope of this investigation and establish a firm foundation linking WTC_{PM} exposure and respiratory tissue inflammation.

WTC_{PM} was found to induce inflammation in mouse nasal and pulmonary tissues, as evidenced by increased neutrophil influx in NLF and BALF. A typical dose-response is not as clearly visible in *in vivo* studies after single exposures to 125 µg as compared to *in vitro* dose-responses. Considerations for this include particle overloading after a certain dose as well as the nature of a non-homogenous mixture which may result in different response outcomes. Additionally, WTC_{PM} exposure was found to significantly increase alveolar macrophage cell death 30 days post-exposure. Changes in pulmonary macrophage cell populations have the potential to alter long-term immune cell responses to WTC_{PM} [15]. Both acute lung injury (ALI) and acute respiratory distress syndrome (ARDS) are characterized by a robust inflammatory response involving substantial infiltration of PMNs into the lung, which ultimately result in capillary-alveolar barrier dysfunction, followed by pulmonary edema, subsequently resulting in gas exchange dysfunction [13,16]. WTC_{PM} exposure also induced acute proinflammatory mediators and resulted in significantly increased whole lung wet/dry ratios, suggestive of excessive volume of fluid accumulation in the tissue, brought about by aberrant changes in pressures acting across microvascular walls. These changes can provoke epithelial integrity impairment in addition to molecular structural compromises involved in fluid and solute flux.

Inclusively, oxidative stress is known to increase production of inflammatory mediators within epithelial lung cells and immune cells, initiating and/or promoting mechanisms of disease, and has been described as a major contributing mechanism resulting in pathological outcomes associated with respiratory dysfunction [17,18]. What largely remains unknown is how oxidative stress mechanisms impact the nasal-pulmonary region, which remains especially true for WTC exposed cohorts. Under normal homeostatic conditions, reactive oxygen species are generated as byproducts of oxygen metabolism, with reactive nitrogen species generated as products of NO metabolism, and more specifically, nitrite production via oxidation of NO [19]. Cohen et al. identified the potential for a single high exposure to WTC_{PM} to alter pulmonary expression of genes associated with oxidative stress and immune function [20]. Within this investigation, WTC_{PM} was found to induce the nitric oxide (NO) metabolite NO₂⁻ *in vitro* in a dose dependent manner. *In vivo*, WTC_{PM} exposure produced decreased levels of mouse NLF and BALF NO₂⁻, an endpoint associated with pulmonary arterial hypertensive states [21–23]. Concurrently, pulmonary arteriopathy was found to be present in 58% of lung biopsies from non-FDNY WTC-PM exposed individuals [24]. Levels of NO₂⁻ were noted to be doubled in WTC_{PM} exposed mice 90 days post-exposure and may be a consequence of prolonged inflammatory responses including overproduction of nitric oxide (NO) and tissue injury brought about by the dust. This increase in NO₂⁻ has been correlated with asthmatic phenotypes [25,26]. Similarly, asthma and other respiratory-related conditions were found to be new onset cases brought about by exposure to WTC_{PM}

in both adults and children [27–31]. While both pulmonary arteriopathy and asthmatic pathologies have markedly different clinical presentations, they share key pathological features (inflammation and smooth muscle cell constriction and proliferation), thought to be a consequence of either mechanical distal airway compression via remodeled pulmonary arteries or imbalances in vaso/broncho-constrictive mediators (increased endothelin-1 and decreased NO) [32,33].

Cardiovascular diseases are among the emerging health concerns from WTC_{PM} exposure [34–36]. NO, a product of endothelial NO synthase (eNOS) and a key signaling molecule involved in vascular homeostatic processes was found to be significantly decreased in serum NO₂⁻ 24 hours post-exposure. Conversely, mouse serum NO₂⁻ levels more than doubled 90 days post-WTC_{PM} exposure, mirroring NO₂⁻ level activities in NLF and BALF samples. Decreases in NO bioavailability have been found to be a hallmark feature in endothelial dysfunction preceding atherosclerotic events as well as an independent predictor of cardiovascular risk, attributed to NO synthesis reduction and reduced NO scavenging by ROS [37]. On the contrary, endothelial dysfunction has been associated with eNOS upregulation rather than downregulation, attributed to elevated levels of H₂O₂, a dismutation product of O₂⁻ [38,39]. The vascular myography studies herein suggest WTC_{PM} can induce endothelial dysfunction over time, given evidence of NO₂⁻ dysregulation and pharmacologic testing of vascular tone through vasoconstrictive and vasorelaxation mechanisms.

Due to the high alkaline nature of WTC_{PM}, it is important to discern whether exposure outcomes were driven by the presence of WTC particles or by the alkaline nature of the dust. Neutralized particles resulted in a doubling of % PMN influx into WTC_{PM} exposed lungs of mice as compared to animals exposed to WTC_{PM} suspended in water. Lending more evidential support for particle driven outcomes, neutralized particles independently induced increased NO₂⁻ production in mouse nasal cavities while simultaneously depleting levels of NO₂⁻ in lower airway tissues. What remains unanswered is why do neutralized WTC particles induce a larger inflammatory response? Metals identified in WTC_{PM} have been found to have long retention times in rat pulmonary tissues [40]. Multiple studies have identified metal solubility to increase with lower pH environments. Physiologically, these environments can be found within cellular lysosomal compartments. Hypothetically, solubilized metal ion release from lysosomal compartments into extracellular fluids may incite inflammatory pathways that would otherwise be kept in homeostatic balance. The addition of an acutely alkaline pH environment may hinder lysosomal capacities to degrade internal compartmental contents, resulting in a less robust inflammatory response.

It is important to note WTC_{PM} exposure was done using a novel technique with suspended WTC_{PM} delivered through IN instillation, providing the most optimal exposure scenario with relevance to both nasal and pulmonary tissues, as well as mimicking the significantly high incidence of particle overloading that occurred in those caught in the dense WTC_{PM} plume. Inhalation is a natural delivery mechanism for particles and has led to comparable/real world exposure scenarios, allowing for evaluations at all levels of the respiratory tract as well as deposition, clearance, kinetics, and calculated delivered dose studies [41, 42]. The largest limitation of inhalation studies, in comparison to studies presented here, is inhalation studies largely apply to fine and ultrafine fractions of particles. Due to the presence of much

larger sized particles in WTC_{PM}, these larger particles may deposit on the outer nares of mice or clog their nasal passages, producing impacts mostly in the upper respiratory tract, limiting particle delivery to the lungs and other targets. Thus, particle suspensions were used, allowing for particles to be more equally distributed throughout the nasal cavity, as well as aspirated into the lower respiratory tract, reaching the lungs not as a sheet of liquid but rather aerosolized as large droplets and deposited in the lung as individual particles. However, it is important to recognize that the use of particle suspensions has its own limitations. During inhalation, particles are delivered as individual particles, which when deposited, have direct contact/ hits with epithelial surfaces. In the case of highly alkaline WTC_{PM}, this mode of deposition could produce intense, localized alkaline spots that could be more injurious than when in suspension. Using suspended particles, the impact of initial hits on airway epithelium may be reduced, potentially underestimating both acute and chronic outcomes from exposure to WTC_{PM}.

Conclusion

Most available data on WTC_{PM} exposed human cohorts have been from epidemiologic studies, with limited literature investigating causative mechanisms of disease. This investigation serves as the first study to systematically explore the particle-driven inflammatory effects of WTC_{PM}, as well as providing the first extensive data on acute and subchronic systemic responses related to WTC_{PM} exposure. These data further validate the toxic potential of a dust that was initially considered to be “harmless”, putting the health of the public at great risk, especially for rescue workers, cleanup crews, and local residents who were continuously exposed.

This study has demonstrated WTC_{PM} exposure alone to be an inducer of nitritive stress and inflammation in nasal, pulmonary, and to some extent cardiovascular tissues. In addition, *in vitro* studies using pulmonary and monocytic immune cell lines revealed increased susceptibility to cell injury and death in relation to WTC_{PM} exposure. Implications for other adverse health outcomes could include further cardiovascular homeostatic alterations as well as mental health outcomes, due to the location and proximity of CNS tissues (olfactory receptor neurons) in the nasal cavity. In addition, insoluble WTC_{PM} deposited on epithelial linings were not fully cleared, resulting in tissue particle retention. Subsequent particle translocation via anterograde transport by olfactory receptor neurons or organ-to-systemic distribution pathways should be investigated further.

Supplementary Material

Refer to Web version on PubMed Central for supplementary material.

Acknowledgements:

Authors acknowledge Dr. Mitchell Cohen for his detailed critical review of this manuscript. Authors would also like to acknowledge the following persons for their courageous task of collecting WTC dust samples on September 12th and 13th near Ground Zero. The field team was led by Dr. Mitchell Cohen and consisted of: M. Blaustein, SI Hsu, J Duffey, J Clemente, K Schermerhom, G Chee, C Prophete, and J Gorczynski.

Funding: This research was supported by NYU's National Institute of Environmental Health Sciences Center of Excellence (ES000260), and Training Grants (T32ES007324, F31ES 025591).

Toxicol Appl Pharmacol. Author manuscript; available in PMC 2021 August 01.

Table of Abbreviations

Abs	Absorbance
Ach	Acetylcholine
Ag	Silver
Al	Aluminum
ANOVA	Analysis of Variance
As	Arsenic
ATCC	American Type Culture Company
Ba	Barium
BALF	Bronchoalveolar Lavage Fluid
Be	Beryllium
BEAS-2B	Immortalized Human Bronchial Epithelial Cells
C57BL/6	C57BL/6 Inbred Mouse
Ca	Calcium
Cd	Cadmium
CD-X	Cluster of Differentiation
CNS	Central Nervous System
Co	Cobalt
COPD	Chronic Obstructive Pulmonary Disease
Cr	Chromium
Cu	Copper
DMEM	Dulbecco's Modified Eagle Medium
DMSO	Dimethyl Sulfoxide
DPBS	Dulbecco's Phosphate Buffered Saline
ELISA	Enzyme-Linked Immunosorbent Assays
FBS	Fetal Bovine Serum
Fe	Iron
G-CSF	Granulocyte-colony stimulating factor
GM-CSF	Granulocyte-Macrophage Colony Stimulating Factor

H&E	Hematoxylin and Eosin
HCl	Hydrochloric Acid
IACUC	Institutional Animal Care and Use Committee
ICP-MS	Inductively Coupled Plasma Mass Spectrometry
In	Indium ICP-MS Internal Standard
IN	Intranasal
iNOS	Inducible Nitric Oxide Synthase
IT	Intratracheal Instillation
K	Potassium
KO	Knock Out Mouse
KPSS	High Potassium Physiologic Salt Solution
LDH	Lactate Dehydrogenase
Mg	Magnesium
Mn	Manganese
Mo	Molybdenum
mRNA	Messenger Ribonucleic Acid
Na	Sodium
NaOH	Sodium Hydroxide
Ni	Nickel
NLF	Nasal Lavage Fluid
NO	Nitric Oxide
NO₂⁻	Nitrite
P/S	Penicillin/Streptomycin
PAS	Periodic Acid Schiff
Pb	Lead
PE	Phenylephrine
PM	Particulate Matter
PM_{2.5}	Particulate Matter <2.5µm
PM₁₀	Particulate Matter <10µm

PMA	Phorbol-12-Myristate-13-Acetate
PMN	Polymorphonuclear Neutrophil
PSS	Physiologic Salt Solution
ROS	Reactive Oxygen Species
Sb	Antimony
Sc	Scandium ICP-MS Internal Standard
Se	Selenium
SEM	Standard Error Mean
Sn	Tin
Sr	Strontium
Tb	Terbium ICP-MS Internal Standard
THP-1	Human Leukemic Monocyte Line
Ti	Titanium
Tl	Thallium
TNF	Tumor Necrosis Factor
V	Vanadium
WTC	World Trade Center
WTC_{PM}	World Trade Center Particulate Matter
WTC_{PM<2.5}	World Trade Center Particulate Matter <2.5 μm
WTC_{PM10-53}	World Trade Center Particulate Matter 10-53
WTC_{PM<53}	World Trade Center Particulate Matter <53 μm
Zn	Zinc

Bibliography

1. Rom WN, et al., Emerging exposures and respiratory health: World Trade Center dust. *Proc AmThorac Soc*, 2010 7(2): p. 142–5.
2. Chen LC and Thurston G, World Trade Center cough. *Lancet*, 2002 360 Suppl: p. s37–8. [PubMed: 12504497]
3. Lippmann M, Cohen MD, and Chen LC, Health effects of World Trade Center (WTC) Dust: An unprecedented disaster's inadequate risk management. *Crit Rev Toxicol*, 2015 45(6): p. 492–530. [PubMed: 26058443]
4. Liroy PJ, et al., Characterization of the dust/smoke aerosol that settled east of the World Trade Center (WTC) in lower Manhattan after the collapse of the WTC 11 September 2001. *Environ Health Perspect*, 2002 110(7): p. 703–14. [PubMed: 12117648]

5. McGee JK, et al., Chemical analysis of World Trade Center fine particulate matter for use in toxicologic assessment. *Environ Health Perspect*, 2003 111(7): p. 972–80. [PubMed: 12782501]
6. Lohn M, et al., Periadventitial fat releases a vascular relaxing factor. *FASEB J*, 2002 16(9): p. 1057–63. [PubMed: 12087067]
7. Quan C, et al., Comparative effects of inhaled diesel exhaust and ambient fine particles on inflammation, atherosclerosis, and vascular dysfunction. *Inhal Toxicol*, 2010 22(9): p. 738–53. [PubMed: 20462391]
8. Weiden MD, et al., Comparison of WTC dust size on macrophage inflammatory cytokine release in vivo and in vitro. *PLoS One*, 2012 7(7): p. e40016. [PubMed: 22815721]
9. Lambrousis CG, et al., Indications of Potential Toxic/Mutagenic Effects of World Trade Center Dust on Human Lung Cell Cultures. *Online Journal of Biological Sciences*, 2009 9(3): p. 81–95.
10. Gavett SH, et al., World Trade Center fine particulate matter causes respiratory tract hyperresponsiveness in mice. *Environ Health Perspect*, 2003 111(7): p. 981–91. [PubMed: 12782502]
11. Cohen M, et al., Impact of acute exposure to WTC dust on ciliated and goblet cells in lungs of rats. *Inhal Toxicol*, 2015 27(7): p. 354–61. [PubMed: 26194034]
12. Vaughan JM, et al., A novel system to generate WTC dust particles for inhalation exposures. *J Expo Sci Environ Epidemiol*, 2014 24(1): p. 105–12. [PubMed: 24220216]
13. Murray JF, Pulmonary edema: pathophysiology and diagnosis. *Int J Tuberc Lung Dis*, 2011 15(2): p. 155–60, i. [PubMed: 21219673]
14. Lee IT and Yang CM, Inflammatory signalings involved in airway and pulmonary diseases. *Mediators Inflamm*, 2013. 2013: p. 791231.
15. Cohen MD, et al., Effects of metal compounds with distinct physicochemical properties on iron homeostasis and antibacterial activity in the lungs: chromium and vanadium. *Inhal Toxicol*, 2010 22(2): p. 169–78. [PubMed: 19757987]
16. Ware LB, Pathophysiology of acute lung injury and the acute respiratory distress syndrome. *Semin Respir Crit Care Med*, 2006 27(4): p. 337–49. [PubMed: 16909368]
17. Weichenthal SA, et al., Fine Particulate Matter and Emergency Room Visits for Respiratory Illness. Effect Modification by Oxidative Potential. *Am J Respir Crit Care Med*, 2016 194(5): p. 577–86. [PubMed: 26963193]
18. Pardo M, et al., Repeated exposures to roadside particulate matter extracts suppresses pulmonary defense mechanisms, resulting in lipid and protein oxidative damage. *Environ Pollut*, 2016 210: p. 227–37. [PubMed: 26735168]
19. Bartsch H and Nair J, Chronic inflammation and oxidative stress in the genesis and perpetuation of cancer: role of lipid peroxidation, DNA damage, and repair. *Langenbecks Arch Surg*, 2006 391(5): p. 499–510. [PubMed: 16909291]
20. Cohen MD, et al., Acute high-level exposure to WTC particles alters expression of genes associated with oxidative stress and immune function in the lung. *J Immunotoxicol*, 2014: p. 1–14.
21. Yang X, et al., Nitric oxide in both bronchoalveolar lavage fluid and serum is associated with pathogenesis and severity of antigen-induced pulmonary inflammation in rats. *J Asthma*, 2010 47(2): p. 135–44. [PubMed: 20170319]
22. Batra J, Chatterjee R, and Ghosh B, Inducible nitric oxide synthase (iNOS): role in asthma pathogenesis. *Indian J Biochem Biophys*, 2007 44(5): p. 303–9. [PubMed: 18341205]
23. Sato M, et al., Increased nitric oxide in nasal lavage fluid and nitrotyrosine formation in nasal mucosa--indices for severe perennial nasal allergy. *Clin Exp Allergy*, 1998 28(5): p. 597–605. [PubMed: 9645597]
24. Caplan-Shaw CE, et al., Lung pathologic findings in a local residential and working community exposed to World Trade Center dust, gas, and fumes. *J Occup Environ Med*, 2011 53(9): p. 981–91. [PubMed: 21860325]
25. Nadif R, et al., Exhaled nitric oxide, nitrite/nitrate levels, allergy, rhinitis and asthma in the EGEA study. *Eur Respir J*, 2014 44(2): p. 351–60. [PubMed: 24791832]
26. Nandan D, et al., Induced sputum nitrite levels correlate with clinical asthma parameters in children aged 7-18 years with mild to moderate persistent asthma. *Journal of Laboratory Physicians*, 2016 8(2): p. 90–95. [PubMed: 27365917]

27. Wheeler K, et al., Asthma diagnosed after 11 September 2001 among rescue and recovery workers: findings from the World Trade Center Health Registry. *Environ Health Perspect*, 2007 115(11): p. 1584–90. [PubMed: 18007989]
28. Lin S, et al., Lower respiratory symptoms among residents living near the World Trade Center, two and four years after 9/11. *Int J Occup Environ Health*, 2010 16(1): p. 44–52. [PubMed: 20166318]
29. Wisnivesky JP, et al., Persistence of multiple illnesses in World Trade Center rescue and recovery workers: a cohort study. *Lancet*, 2011 378(9794): p. 888–97. [PubMed: 21890053]
30. Friedman SM, et al., Case-control study of lung function in World Trade Center Health Registry area residents and workers. *Am J Respir Crit Care Med*, 2011 184(5): p. 582–9. [PubMed: 21642248]
31. Ekenga CC, et al., 9/11-related experiences and tasks of landfill and barge workers: qualitative analysis from the World Trade Center Health Registry. *BMC Public Health*, 2011 11: p. 321. [PubMed: 21575237]
32. Said SI, Hamidi SA, and Gonzalez Bose L, Asthma and pulmonary arterial hypertension: do they share a key mechanism of pathogenesis? *Eur Respir J*, 2010 35(4): p. 730–4. [PubMed: 20356986]
33. Achouh L, et al., Pulmonary arterial hypertension masquerading as severe refractory asthma. *Eur Respir J*, 2008 32(2): p. 513–6. [PubMed: 18669791]
34. Lin S, Gomez MI, Gensburg L, Liu W, Hwang SA. Respiratory and cardiovascular hospitalizations after the World Trade Center disaster. *Arch Environ Occup Health*. 2010a;65:12–20. [PubMed: 20146998]
35. Jordan HT, et al., Cardiovascular disease hospitalizations in relation to exposure to the September 11, 2001 World Trade Center disaster and posttraumatic stress disorder. *J Am Heart Assoc*, 2013 2(5): p. e000431. [PubMed: 24157650]
36. Trasande L, et al., Associations of World Trade Center exposures with pulmonary and cardiometabolic outcomes among children seeking care for health concerns. *Sci Total Environ*, 2013 444: p. 320–6. [PubMed: 23280289]
37. Lin CP, et al., Endothelial progenitor cell dysfunction in cardiovascular diseases: role of reactive oxygen species and inflammation. *Biomed Res Int*, 2013. 2013: p. 845037.
38. Kuboki K, et al., Regulation of Endothelial Constitutive Nitric Oxide Synthase Gene Expression in Endothelial Cells and In Vivo. A Specific Vascular Action of Insulin, 2000 101(6): p. 676–681.
39. Drummond GR, et al., Transcriptional and posttranscriptional regulation of endothelial nitric oxide synthase expression by hydrogen peroxide. *Circ Res*, 2000 86(3): p. 347–54. [PubMed: 10679488]
40. Antonini JM, et al., Persistence of deposited metals in the lungs after stainless steel and mild steel welding fume inhalation in rats. *Archives of Toxicology*, 2011 85(5): p. 487–498. [PubMed: 20924559]
41. Driscoll KE, et al., Intratracheal instillation as an exposure technique for the evaluation of respiratory tract toxicity: uses and limitations. *Toxicol Sci*, 2000 55(1): p. 24–35. [PubMed: 10788556]
42. Osier M and Oberdorster G, Intratracheal inhalation vs intratracheal instillation: differences in particle effects. *Fundam Appl Toxicol*, 1997 40(2): p. 220–7. [PubMed: 9441718]

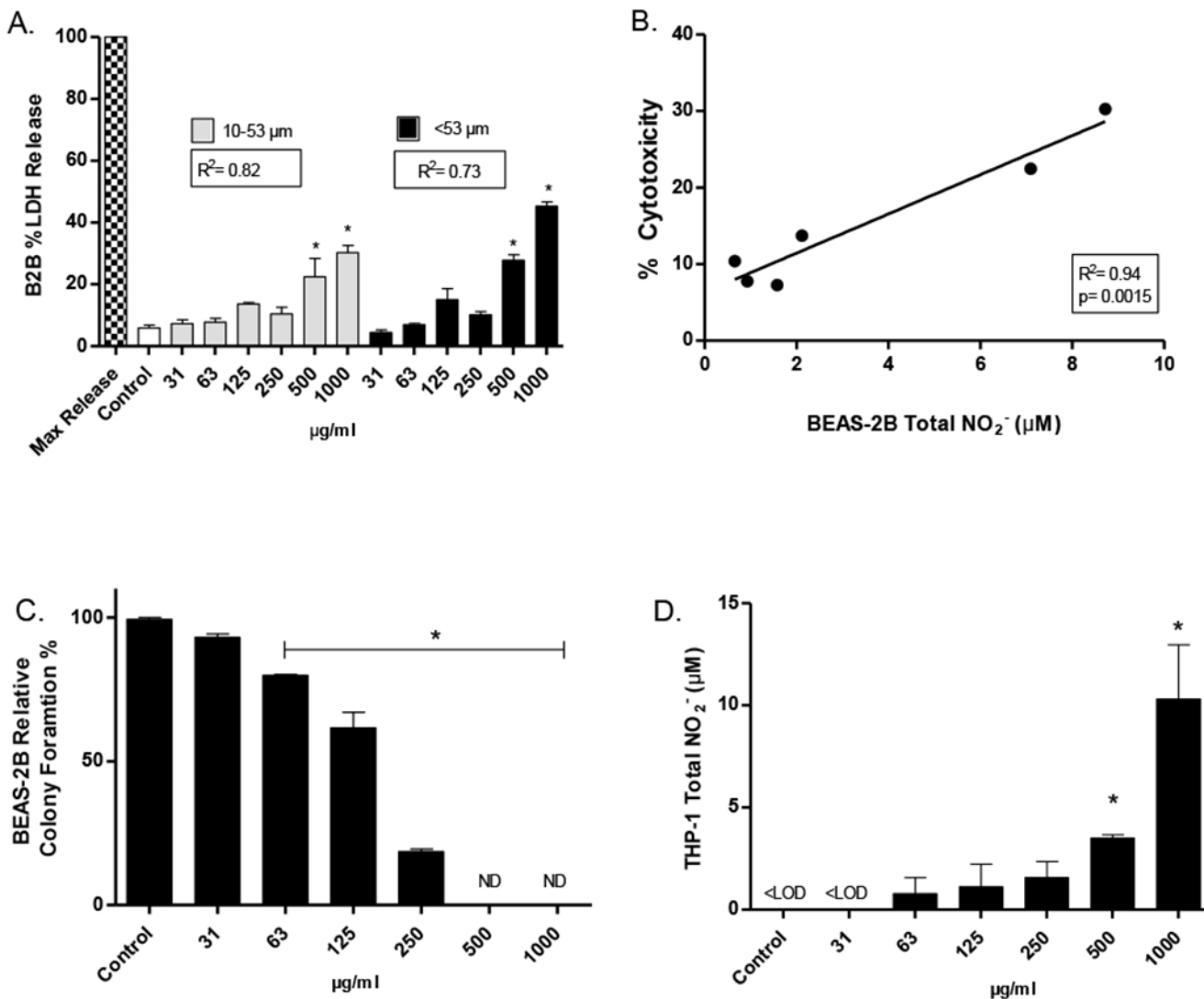


Figure 1. *In vitro* cytotoxicity markers 24 hours post-WTC_{PM} exposure.

A) BEAS-2B lactate dehydrogenase (LDH) release from WTC_{PM10-53 μm} and WTC_{PM<53 μm} exposed cells. Asterisks (*) indicate a statistically significant difference from 1 mg/ml exposures ($p < 0.05$). B) Cytotoxicity and NO₂⁻ correlations with respect to WTC_{PM10-53} exposure. C) Clonogenic survival assay assessment; photos unavailable. D) THP-1 activated monocyte production of NO₂⁻ *in vitro* in relation to WTC_{PM10-53} exposure. Bars are mean ± SEM with $n = 3$ /group. Asterisks (*) indicate a statistically significant difference from control values ($p < 0.05$). <LOD indicates below the limit of detection.

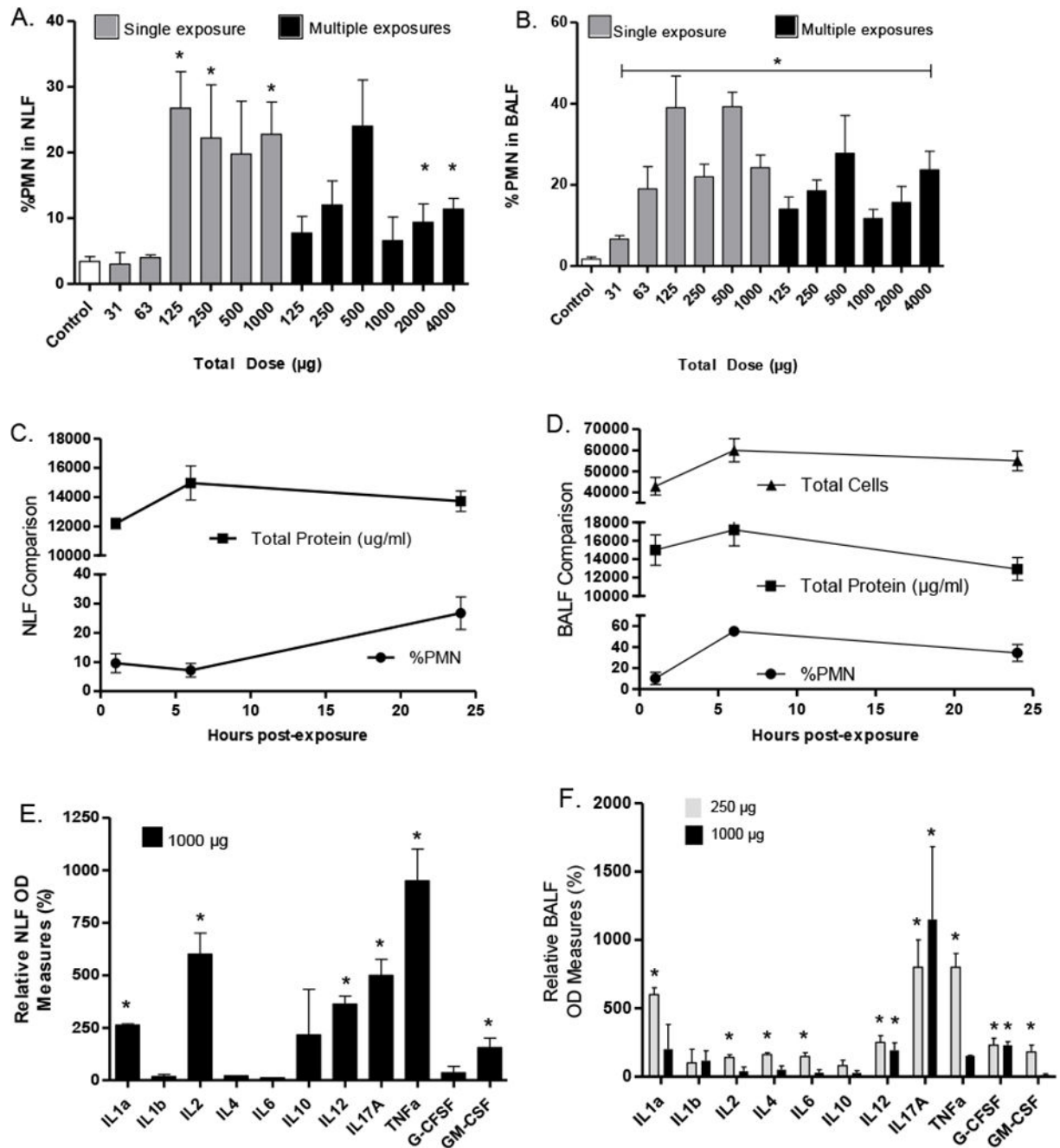


Figure 2. Biomarkers of inflammation in NLF and BALF of $WTC_{PM₅₃}$ exposed C57BL/6 mice. A&B) Percent (%) polymorphonuclear neutrophil (PMN) influx comparisons in NLF and BALF 24 hours post-initial or final $WTC_{PM₅₃}$ exposure. Reported values are averages of individually measured lavage samples \pm SEM with $n=5-7$. C&D) A 24-hour time course comparison of %PMNs, total protein, and total cells in single treatment (125 μ g) mice. Total cell count unavailable for NLF. Time course values are averages of individually measured samples \pm SEM with $n=3-4$. E&F) ELISArray cytokines and chemokines samples were pooled ($n=5$) and measured in duplicate 24 hours post-exposure in NLF and BALF,

respectively (250 µg dose for NLF unavailable). Reported values are relative optical density percentages (relative to control mean values). Asterisks (*) indicate a statistically significant difference from control values ($p < 0.05$).

Author Manuscript

Author Manuscript

Author Manuscript

Author Manuscript

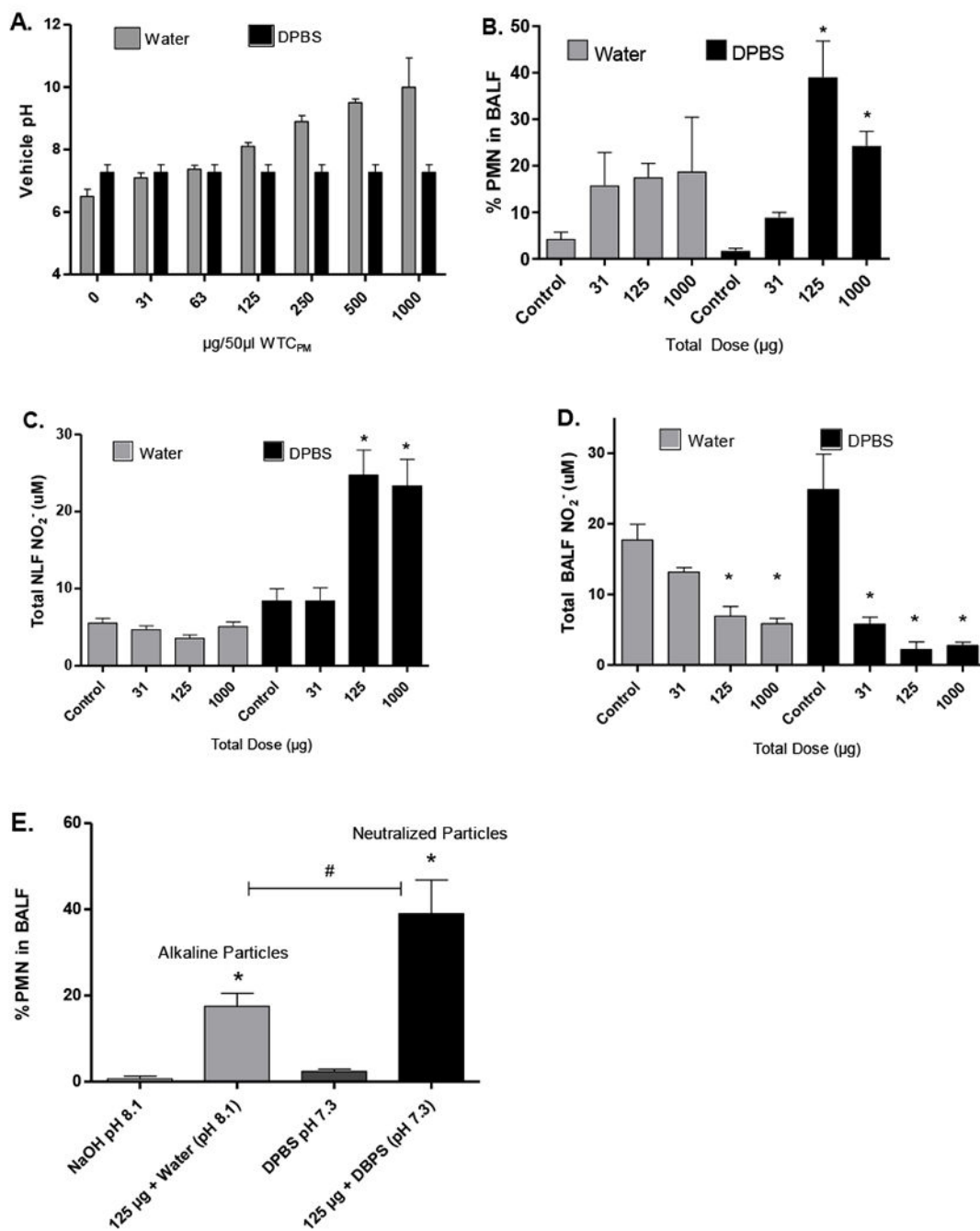


Figure 3. Evaluation of pH and/or particle effect in BALF.

A) pH of WTC_{PM} suspended in water or DPBS at varying concentrations. B) %PMN comparison of water or DPBS suspended WTC_{PM} 24 hours post- single exposure. C&D) NLF and BALF NO₂⁻ evaluation of WTC_{PM} suspended in water or DPBS. Reported values are averages of individually measured samples ±SEM with n=5. E) pH effect vs. particle effect on PMN influx. All endpoints were evaluated 24 hours post single exposure. Symbols (*) and (#) indicate a statistically significant difference from vehicle control values or compared groups, respectively (p<0.05).

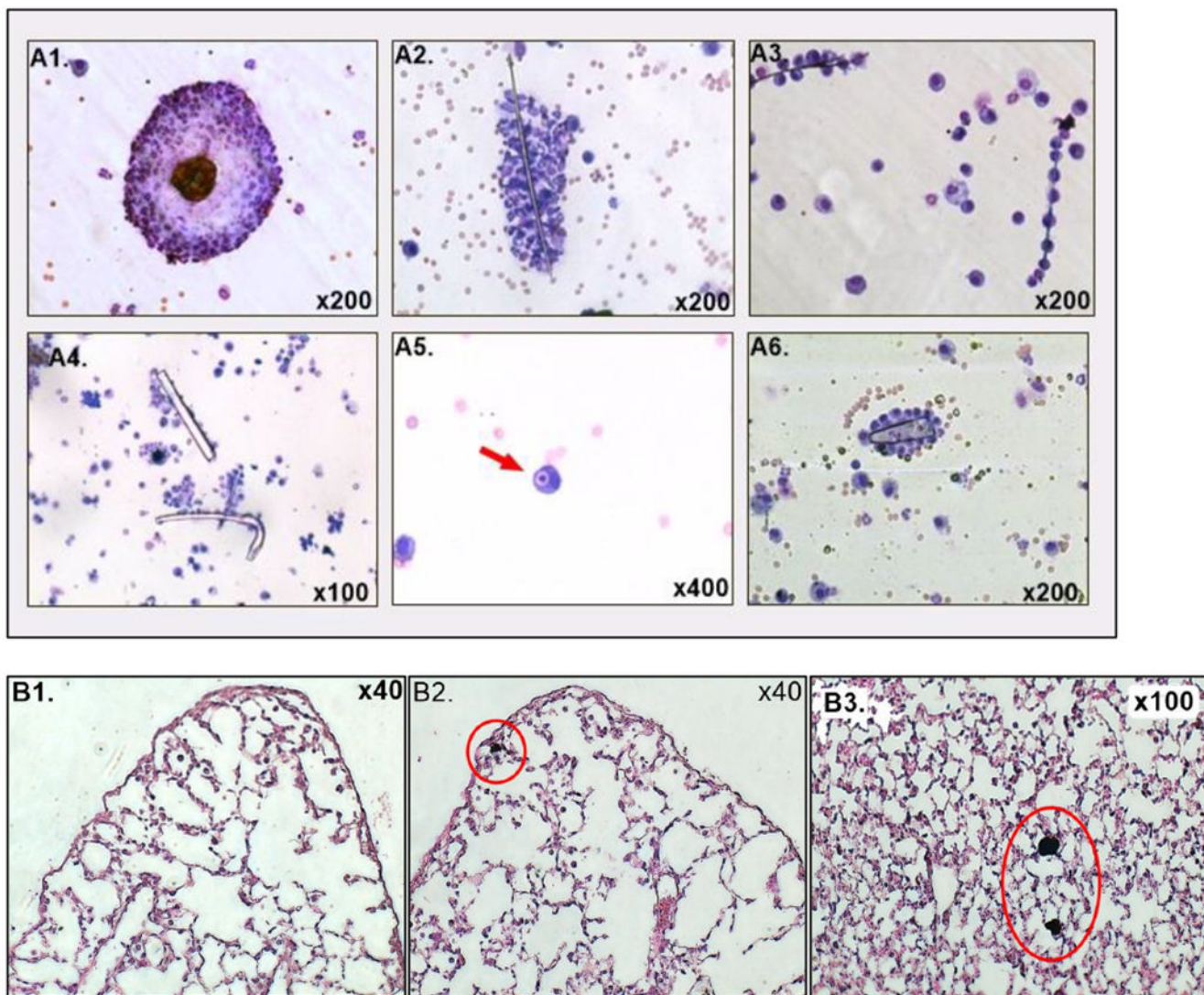


Figure 4. Gross microscopic examination of WTC particles in lavage fluids and pulmonary tissue.

A1-A4) BALF retrieved particles from WTC_{PM<53} exposed mice 24 hours post-exposure. A5) BALF sample; phagosome encapsulated WTC particle within a macrophage. A6) NLF retrieved particles from WTC_{PM<53} exposed mice 24 hours post-exposure. B1-3) Gross histopathological examination of whole lungs and particle retention. H&E staining. Red circles identify embedded WTC particles within pulmonary tissues of WTC_{PM<53} exposed mice.

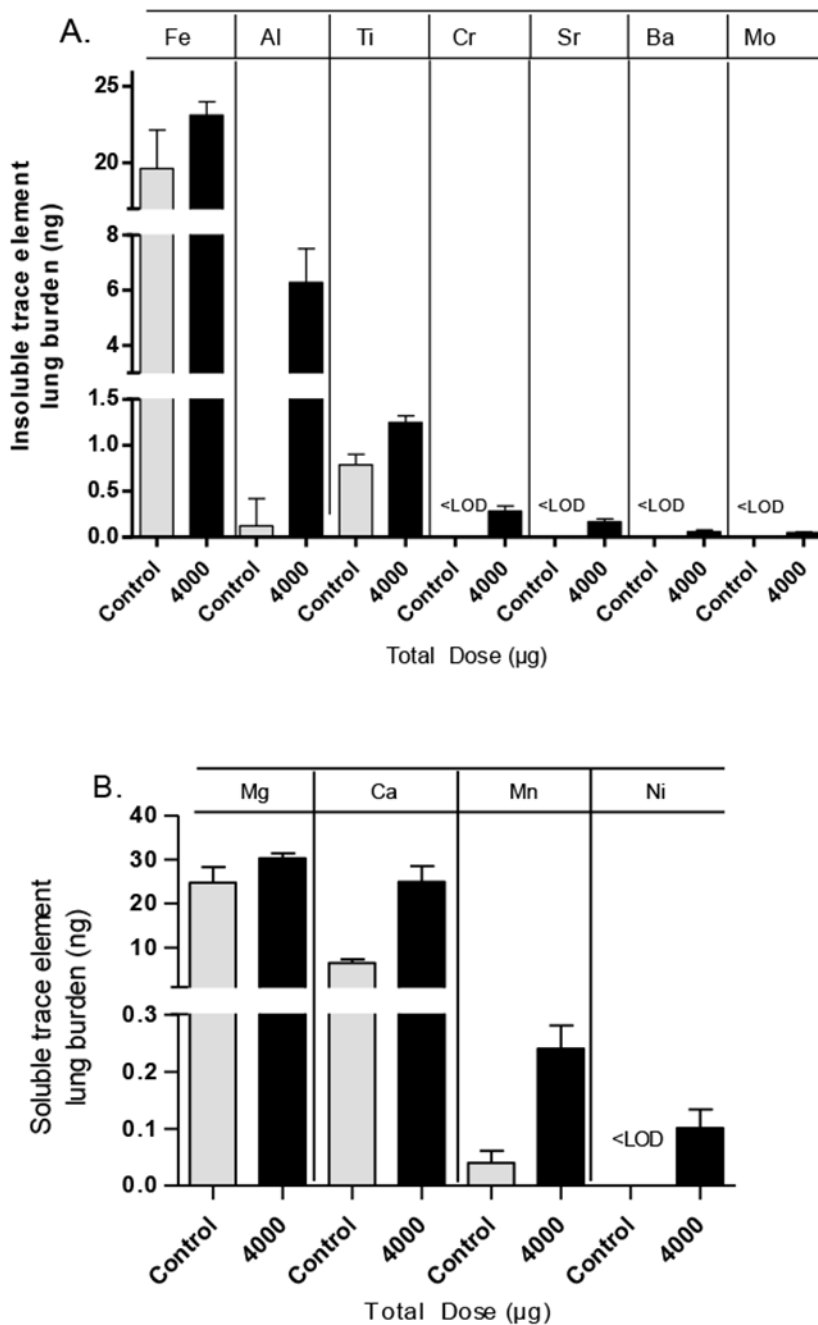


Figure 5. ICP-MS total lung burden of trace elements.

Whole lung analysis of WTC_{PM} exposed mice (4000 µg) 24 hours post-exposure for insoluble (A) and soluble (B) trace elements. All elements presented are statistically significant (p<0.05) in WTC_{PM} exposed mice compared to the control group. Below limit of detection is indicated by <LOD. Reported values are averages of individually measured samples ±SEM with n=4-5.

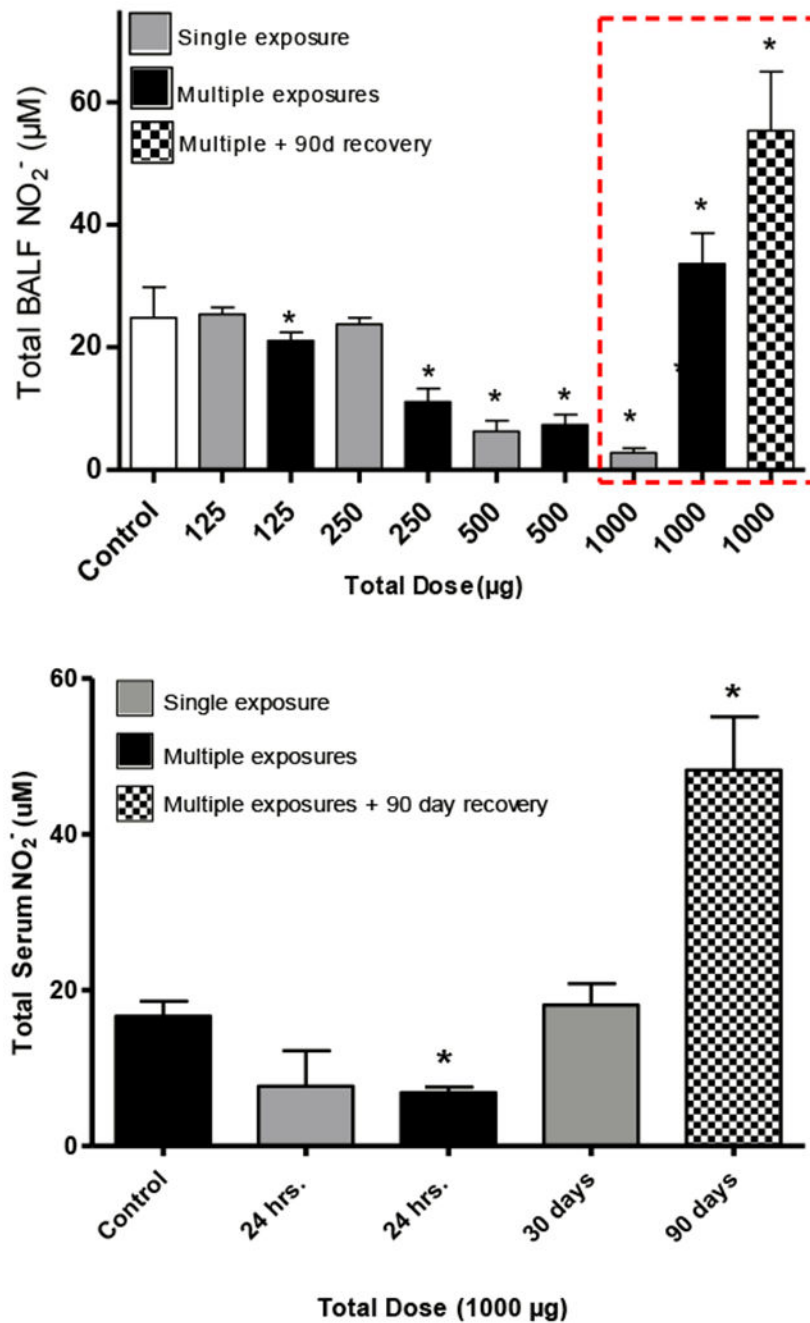


Figure 6. Time course comparisons of BALF and serum NO₂⁻. Doses given as single or multiple dose exposures and evaluated 24 hours, 30 days or 90 days post-exposure. Samples were measured individually in triplicates using the Griess reagent assay. Reported values are averages of individually measured BALF samples \pm SEM with $n=4-6$ and serum samples \pm SEM with $n=3$. Asterisks (*) indicate a statistically significant difference from control values ($p<0.05$).

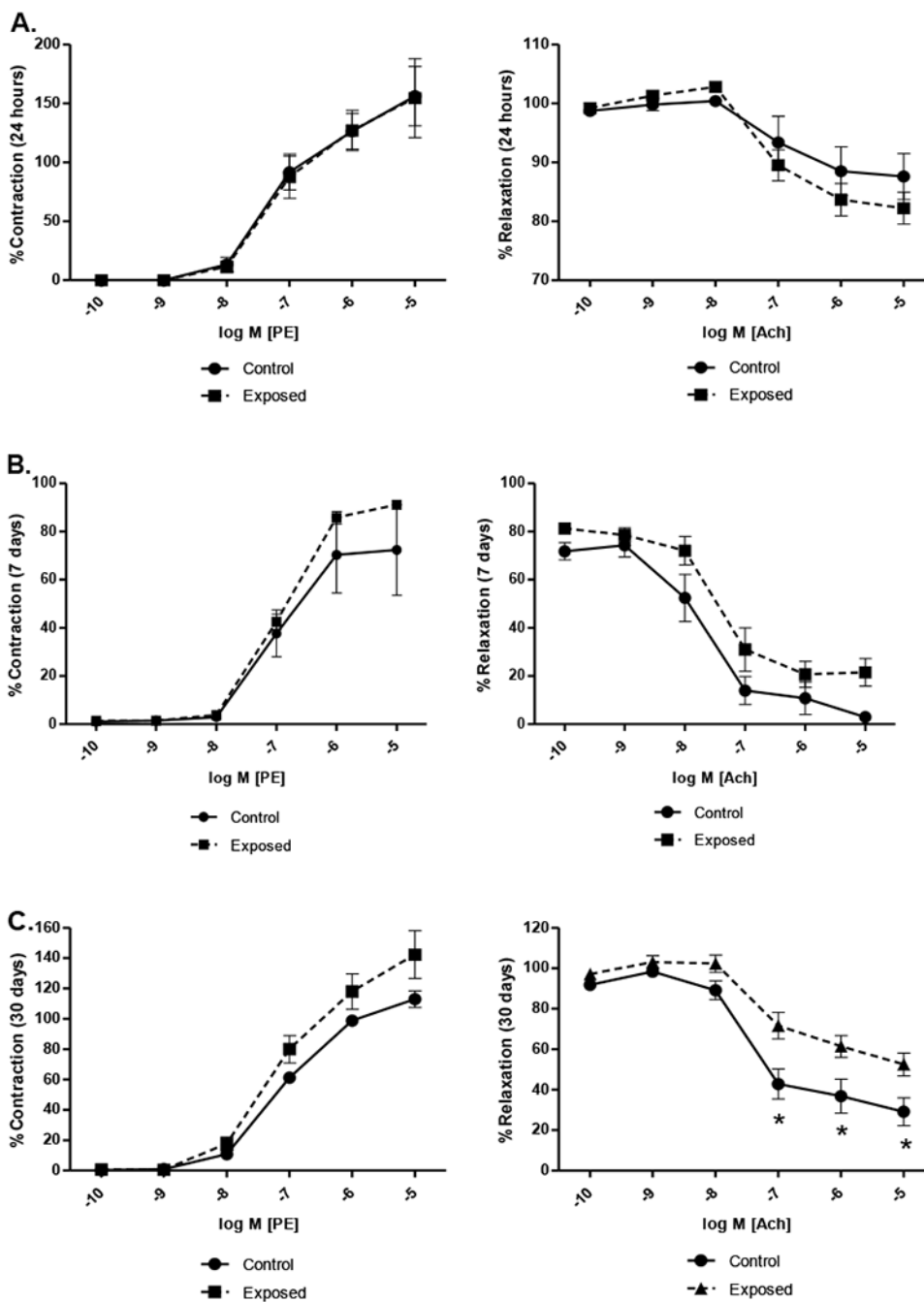


Figure 7. Temporal vascular response curves in response to PE and Ach. Mice were exposed to single dose of 1000 μg WTC_{PM}. Vascular reactivity was measured at 24 hours, 7 days and 30 days post-exposure and analyzed by repeated-measures two-way ANOVA with Bonferroni's post-tests. Reported values are averages of individually measured samples \pm SEM with n=3/4. Asterisks (*) indicate a statistically significant difference from control value responses using 2way ANOVA ($p < 0.05$).

Table 1.
WTC_{PM<53} mouse exposure matrices (A) and human equivalent dosing (HED; B).

HED (mg) calculations and ratios are derived from regulatory allometric body weight scaling factors of 0.67 ($BW^{0.67}$) and 0.75 ($BW^{0.75}$) and assuming an average mouse weight of 0.02 kg and 50 kg or 70 kg for humans.

A.			
Exposure groups	Dosing Frequency	Sacrifice Timepoint	Mean sample size (n=)
Single exposure	Single exposure	24 hours., 7 days, or 30 days post-exposure	5
Multiple Exposures	Four exposures over the course of 7 days, every other day.	24 hours. post-final exposure	5
Multiple IN exposures + 90-day recovery period	Four exposures over the course of 7 days, every other day.	90 days post-final exposure	5

B.				
Mouse IN dose (mg)	Mean HED (mg) ($BW^{0.67}$)	Mean HED (mg) ($BW^{0.75}$)	Mean total HED	Inhalable HED (mg/m³)
0.031	6.6	12.5	9.6	1.0
0.062	13.2	25.1	19.1	1.9
0.125	26.6	50.5	38.6	3.9
0.25	53.2	101.1	77.2	7.7
0.5	106.5	202.1	154.3	15.4
1	213.0	404.3	308.6	30.9
4	851.9	1617.2	1234.5	123.5